

RESEARCH ARTICLE

# miR-146a deficiency in hematopoietic cells is not involved in the development of atherosclerosis

Alberto del Monte<sup>1,2\*</sup>, Ana B. Arroyo<sup>3\*</sup>, María J. Andrés-Manzano<sup>1,2</sup>, Nuria García-Barberá<sup>3</sup>, María S. Caleprico<sup>1</sup>, Vicente Vicente<sup>3</sup>, Vanessa Roldán<sup>3</sup>, Rocío González-Conejero<sup>3\*</sup>, Constantino Martínez<sup>3\*</sup>, Vicente Andrés<sup>1,2\*</sup>

**1** Centro Nacional de Investigaciones Cardiovasculares Carlos III (CNIC), Madrid, Spain, **2** CIBER de Enfermedades Cardiovasculares (CIBER-CV), Murcia, Spain, **3** Servicio de Hematología y Oncología Médica, Hospital Universitario Morales Meseguer, Centro Regional de Hemodonación, Universidad de Murcia, IMIB-Arrixaca, Murcia, Spain

\* These authors contributed equally to this work.

\* [rocio.gonzalez@carm.es](mailto:rocio.gonzalez@carm.es) (RG-C); [constant@um.es](mailto:constant@um.es) (CM); [vandres@cnic.es](mailto:vandres@cnic.es) (VA)



## OPEN ACCESS

**Citation:** del Monte A, Arroyo AB, Andrés-Manzano MJ, García-Barberá N, Caleprico MS, Vicente V, et al. (2018) miR-146a deficiency in hematopoietic cells is not involved in the development of atherosclerosis. PLoS ONE 13(6): e0198932. <https://doi.org/10.1371/journal.pone.0198932>

**Editor:** Katrin Schröder, Goethe-Universität Frankfurt am Main, GERMANY

**Received:** March 14, 2018

**Accepted:** May 29, 2018

**Published:** June 14, 2018

**Copyright:** © 2018 del Monte et al. This is an open access article distributed under the terms of the [Creative Commons Attribution License](https://creativecommons.org/licenses/by/4.0/), which permits unrestricted use, distribution, and reproduction in any medium, provided the original author and source are credited.

**Data Availability Statement:** All relevant data are within the paper.

**Funding:** This study was supported by research grants from the Instituto de Salud Carlos III and Fondo Europeo de Desarrollo Regional (FEDER) [P14/00253, Red RIC (RD12/0042/0050 and RD12/0042/0028), CIBERCV CB16/11/00405] and 19873/GERM/15 (Fundación Séneca). A.D.M. has a predoctoral contract from the Spanish Ministerio de Economía, Industria y Competitividad (MEIC) (BES-2014-06779) and A.B.A. has a research

## Abstract

### Background

Atherosclerosis involves activation of the IRAK1/TRAF6/NF-κB inflammatory cascade, which is negatively regulated by miR146a. Previous studies showed that the TT genotype of rs2431697, located near the *miR-146a* gene, drives lower miR-146a transcription and predicts adverse cardiovascular events in anticoagulated atrial fibrillation patients. Moreover, systemic miR-146a administration protects mice from atherosclerosis. Here we evaluated the ability of miR-146a expression in the hematopoietic component to regulate atherosclerosis in low-density lipoprotein receptor-null mice (*Ldlr*<sup>-/-</sup>).

### Methods and results

Lethally-irradiated *Ldlr*<sup>-/-</sup> mice transplanted with bone marrow from wild-type or *miR-146a*-null mice were fed an atherogenic diet for 8 and 20 weeks. *Irak1*, *Traf6* and *MIR146A* expression were quantified in thoracic aorta by qRT-PCR and Western blot. Aortic plaque size and composition were characterized by Oil-Red staining and immunohistochemistry and leukocyte recruitment by intravital microscopy. Blood cell counts were similar in fat-fed *Ldlr*<sup>-/-</sup> mice with or without hematopoietic miR-146a expression. However, plasma cholesterol decreased in fat-fed *Ldlr*<sup>-/-</sup> mice transplanted with bone marrow deficient for miR-146a. Finally, aortic atherosclerosis burden and recruitment of leukocytes into the vessel wall were undistinguishable between the two groups, despite higher levels of *Irak1* and *Traf6* mRNA and protein in the aorta of fat-fed mice lacking hematopoietic miR-146a expression.

### Conclusions

miR-146a deficiency exclusively in hematopoietic cells modulates cholesterol levels in plasma and the expression of its targets in the artery wall of fat-fed *Ldlr*<sup>-/-</sup> mice, but does not

fellowship from Sociedad Española de Trombosis y Hemostasia (SETH). The CNIC is supported by the Ministerio de Economía, Industria y Competitividad (MEIC) and the Pro-CNIC Foundation, and is a Severo Ochoa Center of Excellence (SEV-2015-0505). The funders had no role in study design, data collection and analysis, decision to publish, or preparation of the manuscript.

**Competing interests:** The authors have declared that no competing interests exist.

accelerate atherosclerosis. Atheroprotection upon systemic miR-146a administration may therefore be caused by specific effects on vascular cells.

## Introduction

Atherosclerosis is a complex inflammatory process involving several factors and cell types that interact in response to different forms of injury [1]. Together with endothelium and smooth muscle cells, hematopoietic cells play a central role in atherogenesis [2]. Indeed, a key early event in the inflammatory response during atherosclerosis is the adhesion of neutrophils to the vascular endothelium and their recruitment into the injured artery wall. The secretion of neutrophil-derived myeloperoxidase seems to be an important event in vascular injury [3]. More recent research has implicated the production of neutrophil extracellular traps (NETs) in atherogenesis [4], although further research is required to fully define the underlying mechanisms [5]. Other important hemostatic factors in atherosclerosis are monocytes/macrophages, important inflammatory and invasive cells that regulate plaque formation and necrosis [2,6]. As they infiltrate the artery wall, monocytes polarize into different macrophage subsets that play distinct roles in atherosclerosis [7].

MicroRNAs (miRNAs) are small, non-coding RNAs that posttranscriptionally regulate gene expression by promoting mRNA degradation and/or inhibiting mRNA translation [8,9]. Since their discovery, miRNAs have been implicated as key modulators of numerous physiological and pathological processes. Their role in cardiovascular disease has been extensively studied in recent years [10,11]. In particular, miR-146a has an anti-inflammatory function [12] and its expression is regulated by the single-nucleotide polymorphism (SNP) rs2431697; homozygote TT individuals have lower levels of miR-146a than GG individuals [13]. We recently demonstrated that the levels of miR-146a in monocytes may play an important role in the development of cardiovascular adverse events in patients with atrial fibrillation (AF), with rs2431697-TT patients displaying higher risk of developing adverse cardiovascular events [14]. In turn, monocytes from rs2431697-TT individuals have an increased pro-inflammatory response when subjected to inflammatory stress.

A role for miR-146a in atherosclerosis is suggested by its ability to negatively regulate several pro-inflammatory factors that promote disease progression, including Toll-like receptor 4 (TLR4), IL-1 receptor-associated kinase 1 (IRAK1), and TNF receptor-associated protein factor 6 (TRAF6) [15,16]. Moreover, low miR-146a levels in neutrophils are associated with carotid intima-media thickening in patients with systemic lupus erythematosus [17]. Recent mouse studies reveal that apolipoprotein E (ApoE) enhances miR-146a expression in monocytes and macrophages, suppressing NF- $\kappa$ B-mediated inflammation and atherosclerosis, and that systemic delivery of miR-146a mimetic attenuates monocyte/macrophage activation and atherosclerosis in the absence of plasma lipid reduction [18]. Given these recent studies and the relevance of leukocytes in all stages of atherosclerosis, we investigated whether miR-146a deficiency restricted to the hematopoietic compartment can aggravate the development of high-fat diet (HFD)-induced atherosclerosis in mice deficient for the low-density lipoprotein receptor (*Ldlr*<sup>-/-</sup>) at early (8 weeks) and late stages (20 weeks) of disease progression.

## Materials and methods

### Mice and bone marrow transplantation

Animal welfare, and all experimental and other scientific procedures with animals conformed to EU Directive 2010/63EU and Recommendation 2007/526/EC, enforced in Spanish law under Real Decreto 53/2013. In addition, the animal research included in this work was granted a formal ethics approval by the Committees in charge of animal welfare at Centro Nacional de Investigaciones Cardiovasculares Carlos III (OEBA-CNIC) and Universidad de Murcia (CEEa-UM), the Ethics Committee for Research from Universidad Autónoma de Madrid (OH-UAM), the committee from the Animal Protection Area of the Comunidad Autónoma de Madrid (CAM), and the Animal Health Service of the Department of Agriculture and Water from Región de Murcia (DAW-RM). The ethics approval numbers from the legally competent authorities are PROEX 134/14 (CAM) and A13150602 (DAW-RM). The animals were housed in cages in ventilated racks. Cages contained a bed of wood chips and nesting material, and objects for environmental enrichment. All the animals had ad libitum access to food and water. The maximum number of animals per cage was limited to 5. Mice were maintained under controlled environmental conditions (relative humidity: 45–65%; temperature: 20–24 °C) with light/darkness cycles of 12h/12h.

*miR-146a*<sup>-/-</sup> mice (The Jackson laboratory, Bar Harbor, ME) were backcrossed for more than 8 generations in a C57BL/6J CD45.2 background. Irradiation and bone marrow (BM) transplantation was as described [19]. Briefly, *Ldlr*<sup>-/-</sup> CD45.1 mice (8 to 10-week-old, Charles River) were irradiated with 2 doses of 6.5 Gy (10 minutes each, temperature: 37 °C) using a J.L. Shepherd & Associates 1-68A irradiator with a source of 1000 curies of Cs-137. Next day, the animals were injected in the tail vein with 100 µl of BM cells (7 × 10<sup>6</sup>, in saline) obtained from a pool of 4 femurs and 4 tibias of *miR-146a*<sup>-/-</sup> or wild-type (wt) mice (both C57BL/6J CD45.2; 8-week-old). After 4 weeks on a standard diet, transplanted mice were fed HFD for 8 or 20 weeks (10.7% total fat, 0.75% cholesterol, S9167-E010, SSNIFF, Germany). Transplant efficiency was assessed as the percentage of donor CD45.2-immunoreactive cells in the blood of BM recipient mice, assessed by CD45.2 and CD45.1 immunostaining and flow cytometry.

Animals were all euthanized at the end of every experiment by inhalation of carbon dioxide gas.

### Quantification of atherosclerosis burden and immunohistopathology

All quantitative analyses were performed by an investigator blinded to genotype. Atherosclerosis burden was quantified as described [20]. Briefly, mice were euthanized in a CO<sub>2</sub> chamber and the heart and aorta were extracted after *in situ* perfusion with PBS. Tissues were fixed with 4% paraformaldehyde/PBS overnight at 4 °C. Atherosclerosis burden was quantified by computer-assisted morphometric analysis (SigmaScan pro 5, Systat Software Inc., San Jose, CA) of the aortic arch stained with Oil Red O (O0625, Sigma, 0.2% Oil Red O in 80% MeOH) and of hematoxylin/eosin-stained cross-sections from the aortic root; for each mouse, results were the mean of 3 cross-sections. The area of the necrotic core in atheroma plaques was quantified by analyzing hematoxylin/eosin-stained aortic cross-sections (mean of 3 cross-sections per mouse).

### Blood cell counting and biochemical parameters

Blood was extracted from the facial vein and was analyzed to quantify and identify circulating blood cell populations using the PENTRA 80 hematology platform (HORIBA Medical, Madrid, Spain). Plasma was isolated by centrifugation of whole blood (2000g, 15' at room

temperature), and lipid profile was obtained using DIMENSION RxL MAX (Siemens, Munich, Germany).

### Intravital microscopy

Male *Ldlr*<sup>-/-</sup> mice transplanted with BM wt or BM *miR-146a*<sup>-/-</sup> fed HFD for 20 weeks after transplantation were used for cremaster muscle intravital microscopy as previously described [21]. Briefly, once exteriorised, the cremaster muscle was placed onto an optical clear viewing pedestal, cut longitudinally with a high temperature surgical cautery (Lifeline Medical) and held extended at the corners of the exposed tissue using surgical suture. Ten min before image acquisition, antibodies (0.5 µg) antiCD4 (Tonbo), anti-Ly6G (Biolegend) and anti-Ly6C (eBioscience) were injected to label myeloid cell subsets. To maintain the correct temperature and physiological conditions, exposed tissues were perfused continuously with 37°C pre-warmed Tyrode's buffer solution (139 mM NaCl, 3 mM KCl, 17 mM NaHCO<sub>3</sub>, 12 mM Glucose, 3 mM CaCl<sub>2</sub> and 1 mM MgCl<sub>2</sub>). The cremasteric microcirculation was visualized using an AXIO Examiner Z.1 work station (Zeiss) mounted on a 3-dimensional motorized stage (Sutter Instrument) and equipped with a CoolSnap HQ2 camera (Photometrics). An APO 20x NA 1.0 water-immersion objective was used. Slidebook software 5.0 (Intelligent Imaging Innovations) was employed for acquisition and image processing. Three randomly-selected arterioles and venules were analysed per mouse, and T cells/monocytes/neutrophils were considered adherent when no rolling was observed using a reference line perpendicular to blood flow for at least 30 seconds.

### Quantitative real-time-PCR (qRT-PCR)

Total RNA was isolated from thoracic aortas using RNeasy reagent (Molecular Research Center Inc) and was retrotranscribed (100 ng) using the SuperScript<sup>™</sup> III First-Strand Synthesis System (ThermoFisher). MiR-146a cDNA was synthesized using individual miRNA-specific RT primers and the TaqMan<sup>®</sup> MicroRNA Reverse Transcription Kit (ThermoFisher). cDNA was amplified using TaqMan<sup>®</sup> probes (*Irak1*: Mm01193538\_m1, *Traf6*: Mm00493836\_m1) together with TaqMan<sup>®</sup> Universal PCR Master Mix, No AmpErase<sup>®</sup> UNG (ThermoFisher). The 2<sup>-ΔCt</sup> method was used to calculate the relative abundance of mRNA compared with endogenous actin (*Actb*: Mm02619580\_g1) mRNA and of miRNA compared with U6 for miR-146a (Ct = Threshold Cycle; ΔCt = Ct sample gene-Ct endogenous control).

### Western blotting

Protein lysates were obtained from thoracic aortas of BM *miR-146a*<sup>-/-</sup> and BM wt transplanted mice fed with a HFD for 20 weeks. Tissue homogenization was performed using TissueLyser (Qiagen). Normalization was based on the amount of protein loaded. Total protein (20 µg) was separated by SDS-PAGE (8%) in reducing conditions. Gels were transferred onto PVDF membranes (Amersham Hybond P 0.45, GE Healthcare, Barcelona Spain) and blocked for 1 hour in 5% w/v BSA-TBS. Membranes were incubated overnight at 4°C with primary antibodies against human Traf6 (#sc-8409, 1:1,000, Santa Cruz, Heidelberg, Germany), Irak1 (D51G7, 1:1,000, Cell Signalling Technology, Leiden, The Netherlands), and β-actin (AC-15 clone, 1:5,000, Sigma-Aldrich, Madrid, Spain). After washing, membranes were incubated with secondary antibodies labeled with peroxidase (1:10,000, GE Healthcare, Barcelona, Spain). ECL Prime Detection Kit and ImageQuant LAS 4000 Imager (GE Healthcare, Barcelona, Spain) were used for protein detection. Densitometric analyses were performed with ImageJ software (<http://rsb.info.nih.gov/ij/>).

## Statistical analysis

Data are presented as mean  $\pm$  SEM. In experiments with 2 groups, statistical significance was evaluated using a 2-tailed, unpaired Student's *t*-test. For experiments comparing more than one group, a 1 or 2-way ANOVA with the Bonferroni post hoc tests were performed (Graph-Pad Prism software, La Jolla, CA). Differences were considered statistically significant at  $P < 0.05$ .

## Results

### Genetic disruption of miR-146a in hematopoietic cells does not increase diet-induced atherosclerosis in *Ldlr*<sup>-/-</sup> mice

To assess whether miR-146a deficiency restricted to the hematopoietic compartment affects atherosclerosis, *Ldlr*<sup>-/-</sup> mice (CD45.1 background) were transplanted with BM from *miR-146a*<sup>-/-</sup> (BM *miR-146a*<sup>-/-</sup>) or wt (BM wt) mice (both CD45.2 background) (Fig 1A). After one month, *Ldlr*<sup>-/-</sup> mice were examined to evaluate transplant efficiency by quantifying CD45.1 and CD45.2 expression in circulating blood cells. These studies revealed similar transplant efficiency in both experimental groups (Fig 1B). Transplanted mice were then fed a HFD. Analysis of BM *miR-146a*<sup>-/-</sup> and BM wt mice fed normal chow (pre-diet) and HFD (post-diet) revealed no statistically significant between-group differences in body weight (Fig 1C). MiR-146a levels in blood leukocytes were significantly decreased in BM *miR-146a*<sup>-/-</sup> transplanted mice before and after HFD (Fig 1D). Moreover, in agreement with previously published results [22], we found enlarged spleens and pale BM in *miR-146a*<sup>-/-</sup> transplanted mice (Fig 1E).

Circulating blood cell counts and populations were similar in both groups of mice, except for platelets that were significantly reduced in BM *miR-146a*<sup>-/-</sup> after 20 weeks (Fig 2A). Plasma levels of low-density lipoprotein cholesterol (LDL), total cholesterol, and triglycerides increased significantly in both groups of mice fed HFD for 8 weeks compared with their pre-diet values, but no statistically-significant between-group differences were observed (Fig 2B). However, after 20 weeks of HFD, plasma lipid levels significantly decreased in BM *miR-146a*<sup>-/-</sup> mice compared with BM wt mice (Fig 2B). Thus, genetic disruption of miR-146a in hematopoietic cells did not affect body weight, nor blood cell counts and populations, but reduced plasma lipids after 20 weeks of HFD.

We next quantified atherosclerosis burden in fat-fed mice by planimetric analysis of whole-mount Oil Red-O-stained aortic arch (Fig 3A) and hematoxylin/eosin-stained cross-sections through the aortic root (Fig 3B) after 8 and 20 weeks of HFD. As expected, these studies revealed increased atherosclerosis burden in mice of both groups at 20 weeks of HFD compared with 8 weeks of HFD; however, atherosclerosis development at both times of HFD was similar in BM *miR-146a*<sup>-/-</sup> and BM wt mice in all regions (Fig 3). Similarly, lack of miR-146a in hematopoietic cells did not affect the formation of necrotic cores in the atherosclerotic plaques of mice fed HFD for 8 and 20 weeks (Fig 3C).

### Lack of miR-146a in hematopoietic cells does not augment adhesion of leukocytes in fat fed *Ldlr*<sup>-/-</sup> mice

We next evaluated if miR-146a deficiency in the BM compartment may affect the recruitment and adhesion of leukocytes to the inflamed vessel wall of *Ldlr*<sup>-/-</sup> mice fed HFD for 20 weeks. For this purpose, we analyzed by intravital microscopy the *in vivo* adhesion of labeled leukocytes (Ly6C<sup>+</sup> monocytes, Ly6G<sup>+</sup> neutrophils, and CD4<sup>+</sup> T cells) to the endothelium of cremaster muscle venules. These studies revealed no differences in the adhesion of the different subtypes of leukocytes between BM *miR-146a*<sup>-/-</sup> and BM wt fat-fed *Ldlr*<sup>-/-</sup> mice (Fig 4).



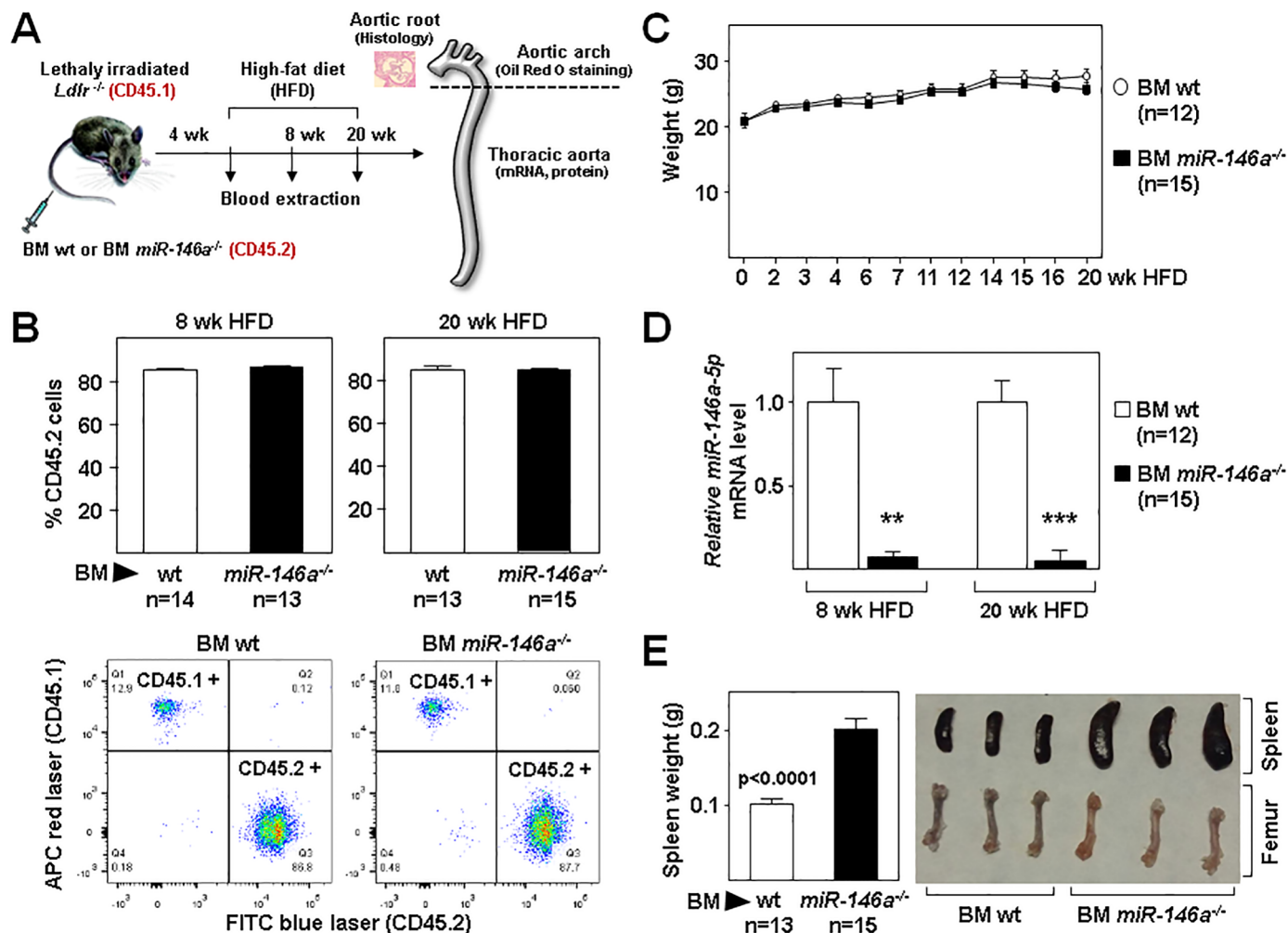


**Fig 1. Study design and efficiency of bone marrow transplantation.** (A) Lethally-irradiated *Ldlr*<sup>-/-</sup> mice (CD45.1, 8 to 10-week-old) were transplanted with cells obtained from bone marrow (BM) of wt or *miR-146a*<sup>-/-</sup> mice (both CD45.2). After 4 weeks of recovery, mice were challenged with a high-fat diet for 8 and 20 weeks. Blood and aorta were collected for biochemical and expression studies and to quantify atherosclerosis burden. (B) Quantification of transplant efficiency in both groups of mice as determined by flow cytometry of blood extracted 1 month after BM transplant. Donor and host cells are CD45.2- and CD45.1- immunoreactive, respectively. Representative flow cytometry profiles are shown below the chart. (C) Body weight at different times after the onset of HFD. (D) Pre and post diet *miR-146a* levels in blood leukocytes were measured by qRT-PCR. The  $2^{-\Delta\Delta C_t}$  method was used to calculate *miRNA* abundance relative to U6 (Ct = Threshold Cycle;  $\Delta C_t$  = Ct sample gene - Ct endogenous control). \*\*: p<0.01, \*\*\*: p<0.001 BM wt vs BM *miR-146a*<sup>-/-</sup> at both time points. (E) Spleen from BM wt or BM *miR-146a*<sup>-/-</sup> mice were weighed after 20 weeks of HFD. Shown are representative images of spleens and femurs.

<https://doi.org/10.1371/journal.pone.0198932.g001>

## Expression of miR-146a targets in fat-fed mice

Thoracic aortas were homogenized and RNA extracted. As expected, the level of *miR-146a* was lower in tissue from fat-fed BM *miR-146a*<sup>-/-</sup> mice compared with BM wt mice at both times of HFD (Fig 5A). Accordingly, mRNA levels of the *miR-146a* targets *Traf6* and *Irak1* were significantly higher in thoracic aortas of BM *miR-146a*<sup>-/-</sup> mice after 8 weeks of HFD (Fig 5B). Similarly, *Traf6* and *Irak1* protein levels were significantly higher in thoracic aortas of BM *miR-146a*<sup>-/-</sup> mice after 20 weeks of HFD (Fig 5C).

## Discussion

There is increasing evidence connecting *miRNAs* with the molecular pathophysiological processes leading to atherosclerosis (reviewed in [11,23]). Inflammation plays a pivotal role in all

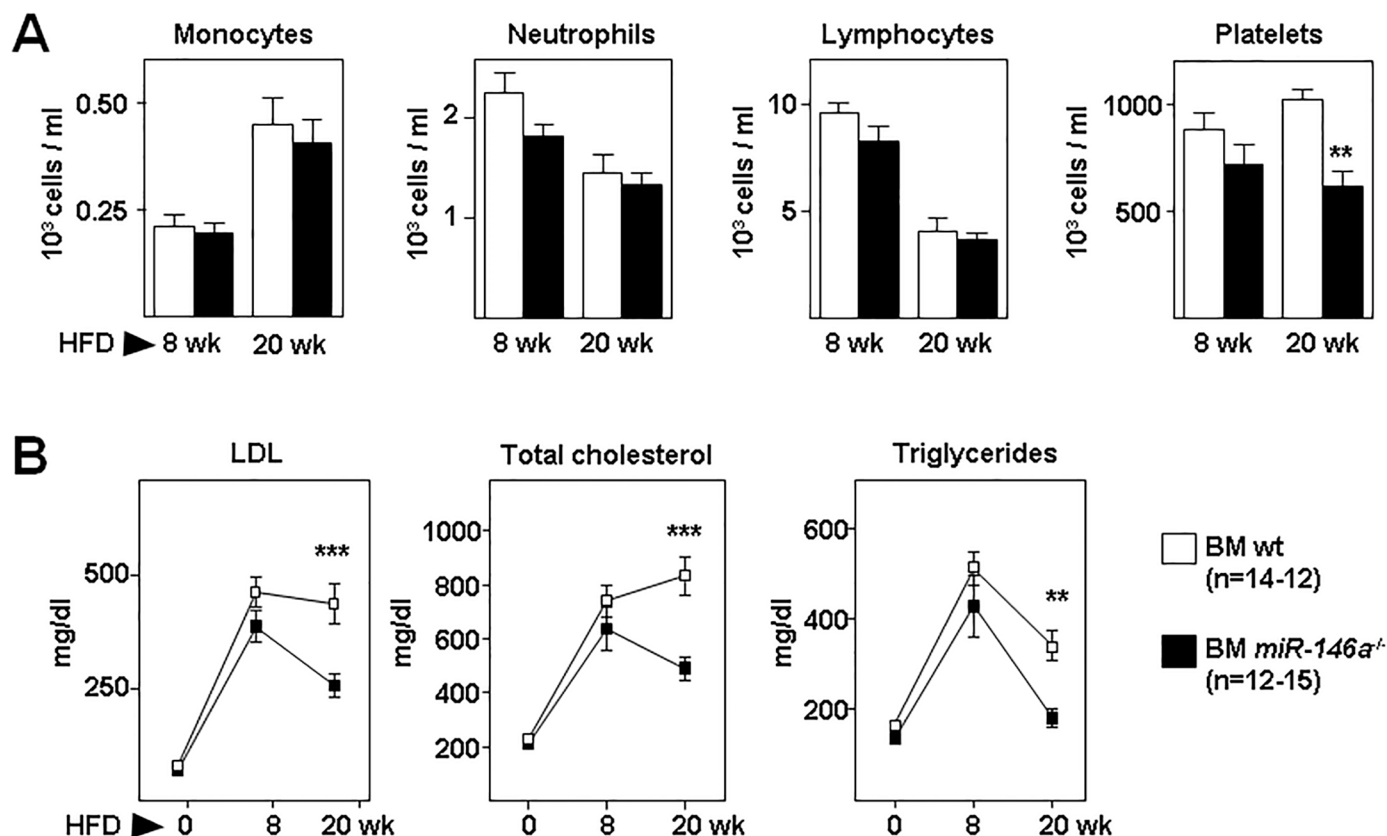


**Fig 2. Hematology and plasma lipids in transplanted *Ldlr*<sup>-/-</sup> mice.** Lethally-irradiated *Ldlr*<sup>-/-</sup> mice (CD45.1, 8 to 10-week-old) were transplanted with cells obtained from bone marrow (BM) of wt or *miR-146a*<sup>-/-</sup> mice (both CD45.2). After 4 weeks of recovery, mice were challenged with a high-fat diet (HFD) for 8 and 20 weeks. **(A)** Blood cell populations from BM wt or BM *miR-146a*<sup>-/-</sup> mice after HFD. **(B)** Plasma levels of LDL, total cholesterol, and triglycerides at 0, 8 and 20 weeks of HFD. \*\*:  $p < 0.01$ , \*\*\*:  $p < 0.001$  BM wt vs BM *miR-146a*<sup>-/-</sup> at 20 weeks of HFD.

<https://doi.org/10.1371/journal.pone.0198932.g002>

stages of atherogenesis, from its initiation until plaque rupture [1,6]. MiR-146a was one of the first miRNAs implicated in inflammatory processes [12]. Through the regulation of different targets of the TLR/NF- $\kappa$ B pathway, miR-146a acts as a negative feedback regulator of the innate immune response [24]. However, the implication of this miRNA in atherosclerosis has been addressed only recently, and several questions remain. Defining the cells in which miR-146a exerts its action will improve understanding of the role of this miRNA in atherogenesis. Recently, Li *et al.* reported that the anti-atherogenic action of ApoE, which is highly expressed in monocytes and macrophages, is mediated through increased expression of the transcription factor PU.1, resulting in enhanced miR-146a expression in monocytes/macrophages and suppression of NF- $\kappa$ B-driven inflammation [18]. These authors also found that systemic delivery of miR-146a mimetic inhibits monocyte/macrophage activation and atherosclerosis development [18]. We observed that lack of miR-146a in the hematopoietic compartment does not affect atherosclerotic plaque formation in *Ldlr*<sup>-/-</sup> mice at early and late stages of disease progression (8 and 20 weeks of HFD). This finding was unexpected because inhibition of the main miR-146a TLR/NF- $\kappa$ B pathway targets in monocytes/macrophages seemed to be protective [18]. Moreover, inhibition of NF- $\kappa$ B activation in macrophages increases atherosclerosis in *Ldlr*<sup>-/-</sup> mice, although surprisingly the opposite occurs in endothelial cells [25]. This was further demonstrated in a model of NEMO/IKKg deletion and upon endothelial cell-specific expression of a dominant-negative I $\kappa$ Ba mutant [26]. Different roles of a TLR/NF- $\kappa$ B

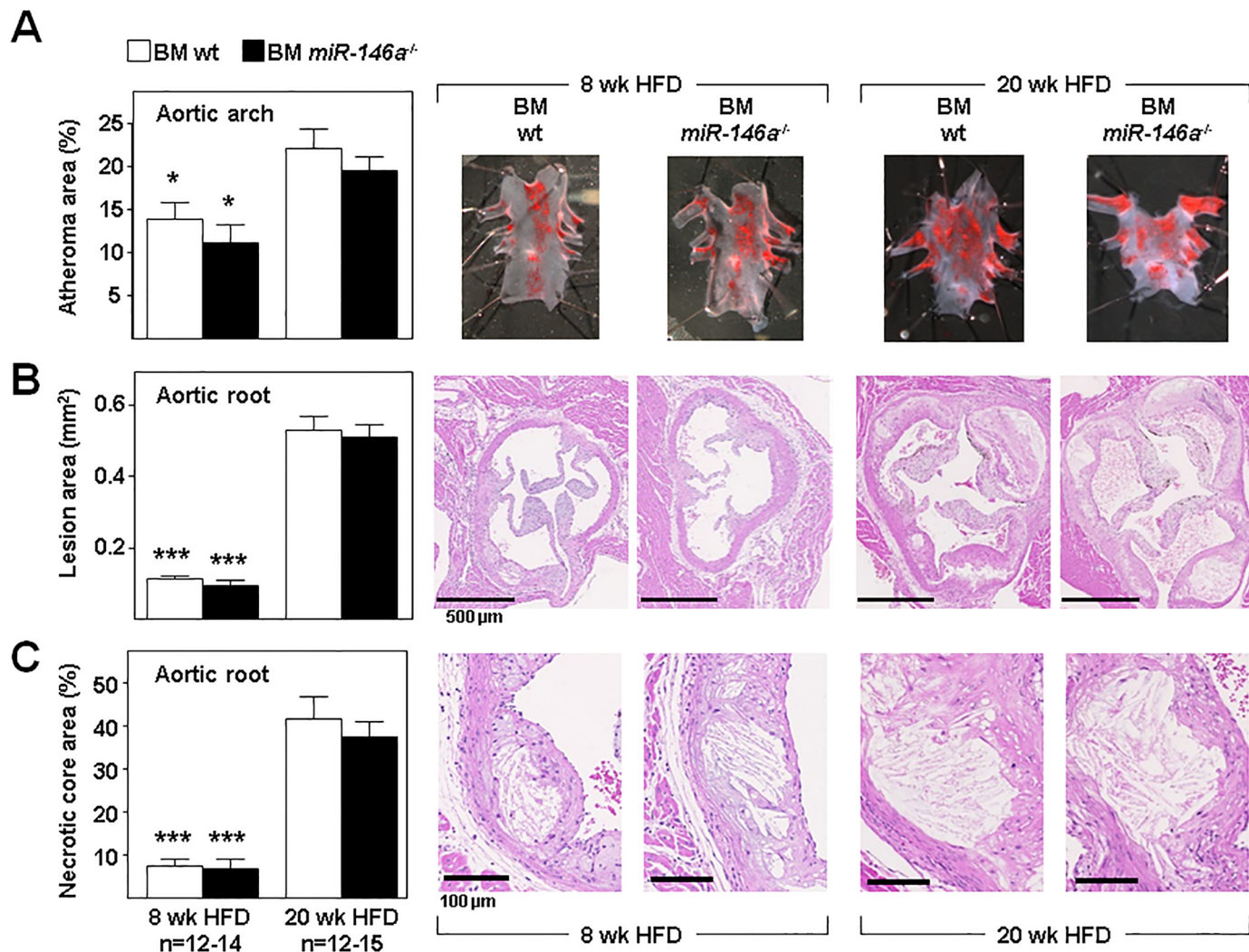


**Fig 3. Ablation of miR-146a gene in hematopoietic cells does not affect diet-induced atherosclerosis in *Ldlr*<sup>-/-</sup> mice.** Lethally-irradiated *Ldlr*<sup>-/-</sup> mice (CD45.1, 8 to 10-week-old) were transplanted with cells obtained from bone marrow (BM) of wt or *miR-146a*<sup>-/-</sup> mice (both CD45.2). After 4 weeks of recovery, mice were challenged with a high-fat diet (HFD). Mice were euthanized after 8 or 20 weeks of HFD and tissues were harvested for immunohistopathological characterization of atherosclerotic lesions. Representative images are shown in each panel. (A) Percentage of aortic arch are occupied by atheroma visualized by *en face* Oil Red O staining. (B) Quantification of atheroma size in hematoxylin/eosin-stained sections of the aortic sinus. (C) Area of atherosclerotic lesions occupied by necrotic cores quantified in histological sections from the aortic sinus. \*:  $p < 0.05$ , \*\*\*:  $p < 0.001$  vs same BM genotype at 20 weeks of HFD.

<https://doi.org/10.1371/journal.pone.0198932.g003>

pathway component in endothelium vs. myeloid cells have also been described for TRAF6 by Polykratis *et al* [27]. These authors showed that endothelial-cell-expressed TRAF6 induces the expression of proinflammatory mediators that enhance the adhesion and recruitment of macrophages to the endothelium, whereas in myeloid cells the opposite occurs, with TRAF6 deficiency favoring the development of atherosclerosis by inhibiting the expression of IL-10 [27]. Our results demonstrate that decreasing the levels of miR-146a in the hematopoietic compartment does not increase atherosclerosis at both early (8 weeks HFD) and late (20 weeks HFD) stages of disease development. Of note, Cheng *et al.* recently showed no differences in atherosclerosis burden in the aortic arch of *Ldlr*<sup>-/-</sup> mice transplanted with BM *miR-146a*<sup>-/-</sup> and fed HFD for 4 weeks; however, they found a significant decrease in plaque burden in BM *miR-146a*<sup>-/-</sup> *Ldlr*<sup>-/-</sup> mice after 12 weeks of HFD [22]. Importantly, these authors observed unchanged



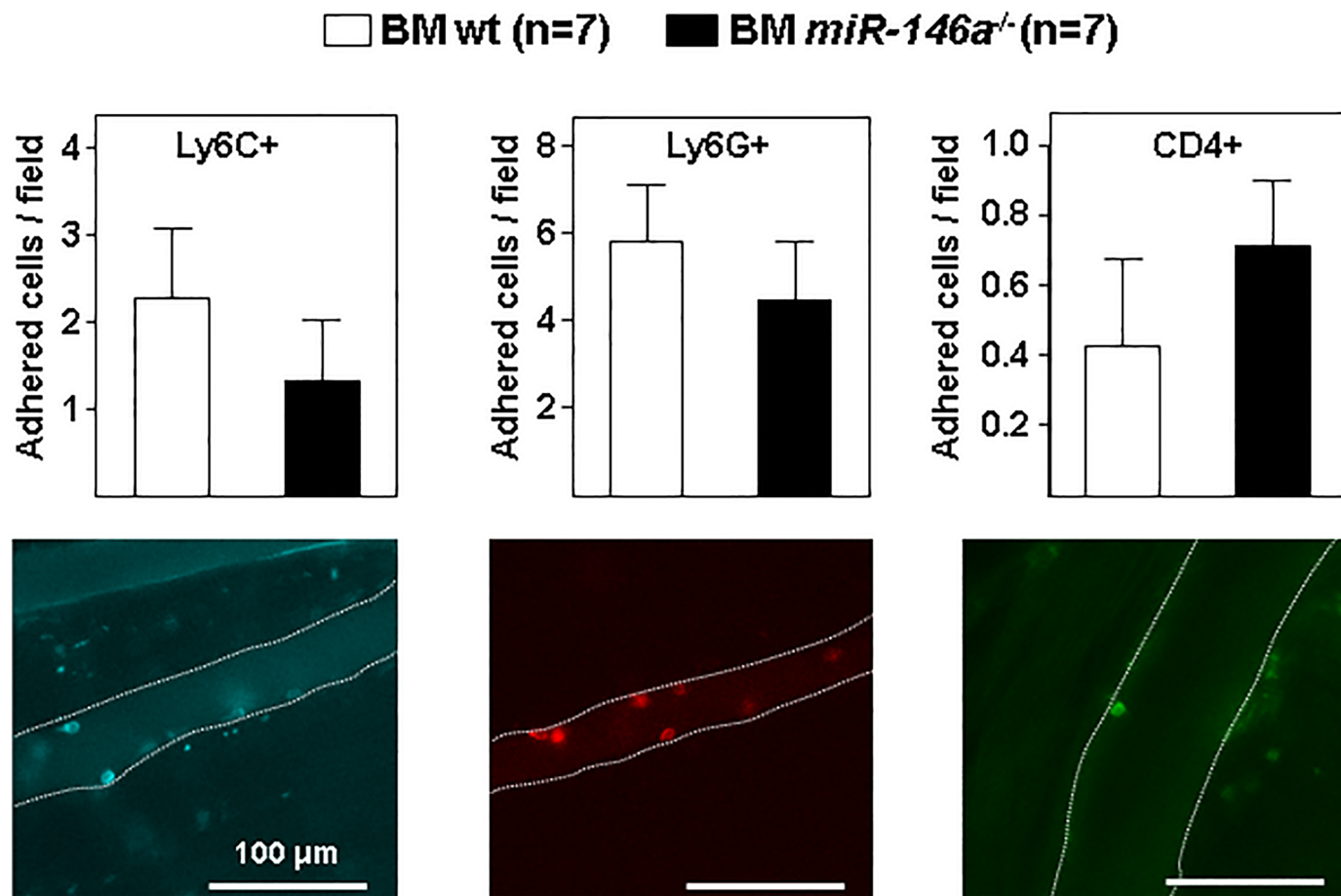


**Fig 4. Deletion of miR-146a gene in hematopoietic cells does not increase adhesion in *Ldlr*<sup>-/-</sup> mice fed HFD.** Lethally-irradiated *Ldlr*<sup>-/-</sup> mice (CD45.1, 8 to 10-week-old) were transplanted with cells obtained from bone marrow (BM) of wt or *miR-146a*<sup>-/-</sup> mice (both CD45.2). After 4 weeks of recovery, mice were challenged with a high-fat diet (HFD) for 20 weeks and analyzed by intravital microscopy in the cremaster muscle. Images are representative for Ly6C<sup>+</sup> monocytes, Ly6G<sup>+</sup> neutrophils, and CD4<sup>+</sup> T cells adhered to the wall of cremasteric venules. Dashed lines mark the boundaries of the venules.

<https://doi.org/10.1371/journal.pone.0198932.g004>

plaque burden in the descending thoracic aorta and aortic root at both time points with HFD. Among other reasons, Cheng *et al.* suggested that low levels of cholesterol after 12 weeks of HFD might explain this atheroprotective role in aortic arch provoked by a miR-146a deficiency in the hematopoietic compartment [22]. We also observed a significant decline in cholesterol after 20 weeks of HFD in BM *miR-146a*<sup>-/-</sup>, but this was not sufficient to reduce plaque burden under our experimental conditions. Consistent with our results showing no differences in atherosclerosis development in fat-fed BM *miR-146a*<sup>-/-</sup> *Ldlr*<sup>-/-</sup> mice, our intravital microscopy studies revealed no differences in vascular leukocyte recruitment upon *miR-146a*<sup>-/-</sup> deficiency in BM cells.

Paradoxically it has also been described that inhibiting miR-146a in endothelial cells may increase the expression of some of its targets, such as TRAF6, thus enhancing NF- $\kappa$ B activation and promoting atherogenesis [28]. Indeed, Cheng *et al.* also demonstrated that mice deficient for miR-146a except in the hematopoietic compartment have a significant increase in atherosclerotic plaque burden in comparison with mice lacking miR-146a in all cells [22]. In line with these results, endothelium-specific delivery of miR-146a-loaded E-selectin-targeting microparticles reduced atherosclerosis in *ApoE*<sup>-/-</sup> mice [29]. In their study of the effect of systemically delivered miR-146a mimetics, Li *et al.* examined expression of endogenous miR-

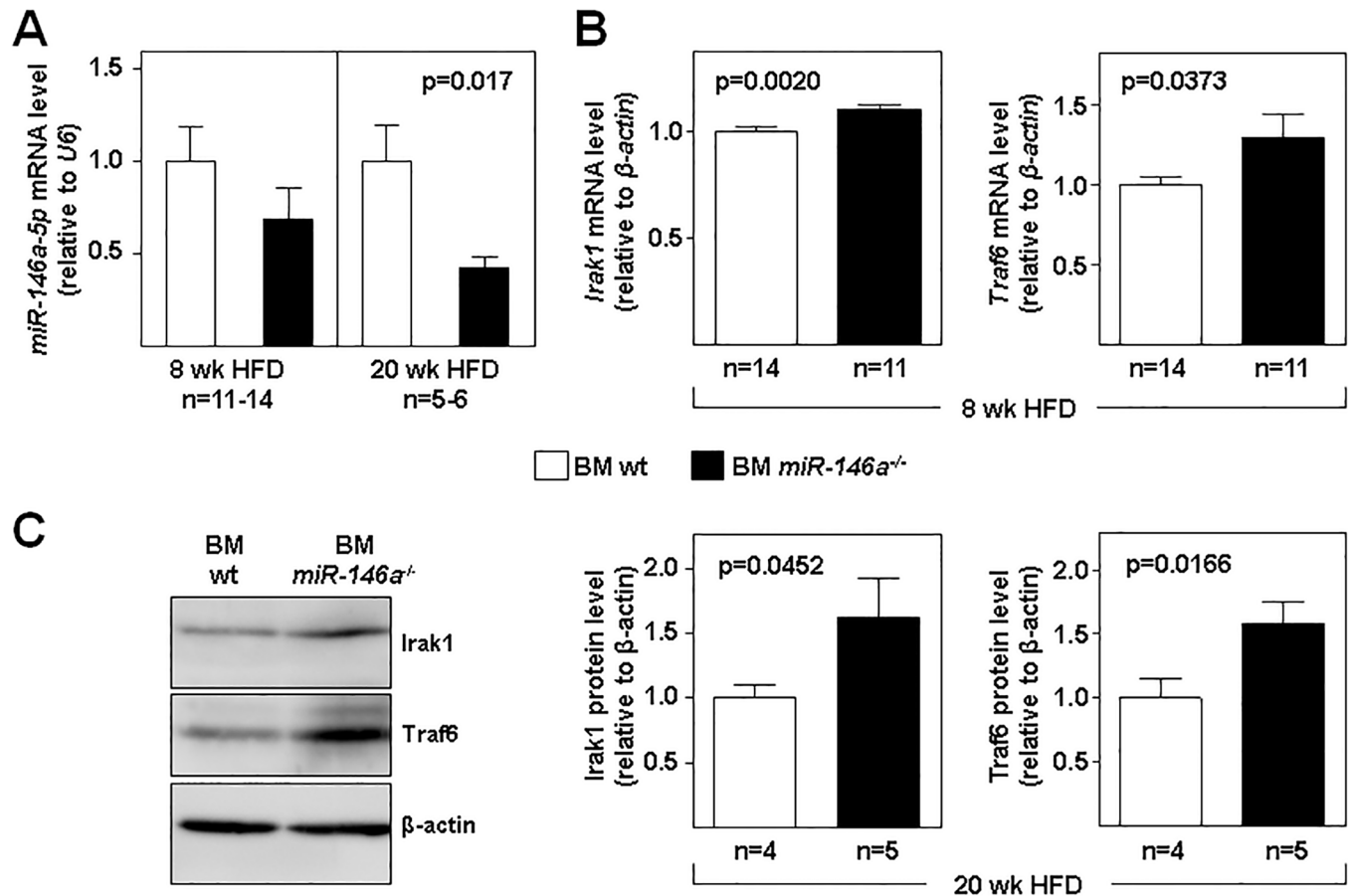


**Fig 5. Expression of *miR-146a* targets in fat-fed mice.** Lethally-irradiated *Ldlr*<sup>-/-</sup> mice (CD45.1, 8 to 10-week-old) were transplanted with cells obtained from bone marrow (BM) of wt or *miR-146a*<sup>-/-</sup> mice (both CD45.2). After 4 weeks of recovery, mice were challenged with a high-fat diet (HFD) for the indicated times. (A) *miR-146a* expression was measured by qRT-PCR in total RNA extracted from the thoracic aorta of mice fed high-fat diet (HFD) for 8 weeks (individual thoracic aortas) and 20 weeks (pools of 3 thoracic aortas per samples). (B) *miR-146a* targets *Irak1* and *Traf6* mRNA levels were measured by qRT-PCR after 8 weeks of HFD. The  $2^{-\Delta Ct}$  method was used to calculate miRNA/mRNA abundance relative to endogenous control expression (U6 in A;  $\beta$ -actin in B) (Ct = Threshold Cycle;  $\Delta Ct$  = Ct sample gene – Ct endogenous control). (C) Representative western blot and quantification of *Irak1* and *Traf6* protein levels (normalized to  $\beta$ -actin) in thoracic aorta of mice receiving BM wt or BM *miR-146a*<sup>-/-</sup> after 20 weeks of HFD (pools of 3 thoracic aortas per sample). \*:  $p < 0.05$ , \*\*:  $p < 0.01$  BM wt vs BM *miR-146a*<sup>-/-</sup> at both time points.

<https://doi.org/10.1371/journal.pone.0198932.g005>

146a in leukocytes, but not in the aorta [18]. It is therefore possible that this treatment increased *miR-146a* levels predominantly in endothelium, as reported for *in vivo* injection of *miRNA* mimetics in other studies [30,31]. Thus, the potential beneficial effect of *miR-146a* in atherosclerosis might be due in part to increased expression in endothelial cells. Thus, despite observing no differences in atherosclerosis burden, we found above-normal expression of specific targets of *miR-146a* such as *Traf6* and *Irak1* in the aorta of BM *146a*<sup>-/-</sup> mice, which exhibited low level of *miR-146a* expression. Since levels of *miR-146a* expression in non-hematopoietic cells are unaffected by BM transplantation, differences in the expression of *miR-146a* and its two targets *Traf6* and *Irak1* might be due to variations in infiltrated leukocytes. Since *miR-146a* deficiency does not increase leukocyte adhesion, leukocyte infiltration should be similar in BM *miR-146a*<sup>-/-</sup> and BM wt mice. Thus, *miR-146a* deficiency in hematopoietic cells affects *miR146a* targets in the inflamed aorta but not sufficiently to aggravate atherosclerosis development in *Ldlr*<sup>-/-</sup> mice. Future studies using conditional *miR146a*-deficient mice for endothelium or vascular smooth muscle cells may help to unequivocally establish this

hypothesis. Additionally, since miR-146a<sup>-/-</sup> mice still express miR-146b, which shares most of the targets with miR-146a, we cannot discard that miR-146b has a compensatory effect in the setting of atherosclerosis model [32]. In conclusion, our results strongly suggest that miR-146a expressed in the hematopoietic compartment plays a negligible role in atherosclerosis development in *Ldlr*<sup>-/-</sup> mice, although its ablation increases in the aorta the proinflammatory state promoted by an atherogenic diet. Identifying how expression of this miRNA limits atherosclerosis remains of high interest. It will therefore be important to develop in vivo models in which to investigate the cells, with special attention to endothelial cells, in which miR-146a exerts its anti-atherogenic function. Finally, investigating the effect of low levels of miR-146a in humans due for example to rs2431697 in atherosclerosis may be of interest to evaluate the clinical impact of a partial miR-146a deficiency.

## Acknowledgments

We thank Simon Bartlett for English editing.

## Author Contributions

**Conceptualization:** Rocío González-Conejero, Constantino Martínez, Vicente Andrés.

**Data curation:** Rocío González-Conejero, Constantino Martínez, Vicente Andrés.

**Formal analysis:** Alberto del Monte, Ana B. Arroyo.

**Funding acquisition:** Rocío González-Conejero, Constantino Martínez, Vicente Andrés.

**Investigation:** Alberto del Monte, Ana B. Arroyo, Rocío González-Conejero, Constantino Martínez, Vicente Andrés.

**Methodology:** Alberto del Monte, Ana B. Arroyo, María J. Andrés-Manzano, Nuria García-Barberá, María S. Caleprico, Rocío González-Conejero, Constantino Martínez, Vicente Andrés.

**Project administration:** Rocío González-Conejero, Constantino Martínez, Vicente Andrés.

**Resources:** Rocío González-Conejero, Constantino Martínez, Vicente Andrés.

**Supervision:** Rocío González-Conejero, Constantino Martínez, Vicente Andrés.

**Writing – original draft:** Rocío González-Conejero, Constantino Martínez, Vicente Andrés.

**Writing – review & editing:** Alberto del Monte, Ana B. Arroyo, Vicente Vicente, Vanessa Rol-dán, Rocío González-Conejero, Constantino Martínez, Vicente Andrés.

## References

1. Lu H, Daugherty A (2015) Atherosclerosis. *Arterioscler Thromb Vasc Biol* 35: 485–491. <https://doi.org/10.1161/ATVBAHA.115.305380> PMID: 25717174
2. Murphy AJ, Tall AR (2016) Disordered haematopoiesis and athero-thrombosis. *Eur Heart J* 37: 1113–1121. <https://doi.org/10.1093/eurheartj/ehv718> PMID: 26869607
3. Tiyerili V, Camara B, Becher MU, Schrickel JW, Lutjohann D, Mollenhauer M, et al (2016) Neutrophil-derived myeloperoxidase promotes atherogenesis and neointima formation in mice. *Int J Cardiol* 204: 29–36. <https://doi.org/10.1016/j.ijcard.2015.11.128> PMID: 26655530
4. Warnatsch A, Ioannou M, Wang Q, Papayannopoulos V (2015) Inflammation. Neutrophil extracellular traps license macrophages for cytokine production in atherosclerosis. *Science* 349: 316–320. PMID: 26185250
5. Soehnlein O, Ortega-Gomez A, Doring Y, Weber C (2015) Neutrophil-macrophage interplay in atherosclerosis: protease-mediated cytokine processing versus NET release. *Thromb Haemost* 114: 866–867. <https://doi.org/10.1160/TH15-08-0623> PMID: 26310276

6. Ross R (1995) Cell biology of atherosclerosis. *Annu Rev Physiol* 57: 791–804. <https://doi.org/10.1146/annurev.ph.57.030195.004043> PMID: 7778883
7. Pello OM, Silvestre C, De PM, Andres V (2011) A glimpse on the phenomenon of macrophage polarization during atherosclerosis. *Immunobiology* 216: 1172–1176. <https://doi.org/10.1016/j.imbio.2011.05.010> PMID: 21802768
8. Bartel DP (2009) MicroRNAs: target recognition and regulatory functions. *Cell* 136: 215–233. <https://doi.org/10.1016/j.cell.2009.01.002> PMID: 19167326
9. Guo H, Ingolia NT, Weissman JS, Bartel DP (2010) Mammalian microRNAs predominantly act to decrease target mRNA levels. *Nature* 466: 835–840. <https://doi.org/10.1038/nature09267> PMID: 20703300
10. McManus DD, Freedman JE (2015) MicroRNAs in platelet function and cardiovascular disease. *Nat Rev Cardiol* 12: 711–717. <https://doi.org/10.1038/nrcardio.2015.101> PMID: 26149483
11. Feinberg MW, Moore KJ (2016) MicroRNA Regulation of Atherosclerosis. *Circ Res* 118: 703–720. <https://doi.org/10.1161/CIRCRESAHA.115.306300> PMID: 26892968
12. Taganov KD, Boldin MP, Chang KJ, Baltimore D (2006) NF-kappaB-dependent induction of microRNA miR-146, an inhibitor targeted to signaling proteins of innate immune responses. *Proc Natl Acad Sci U S A* 103: 12481–12486. <https://doi.org/10.1073/pnas.0605298103> PMID: 16885212
13. Lofgren SE, Frostegard J, Truedsson L, Pons-Estel BA, D'Alfonso S, Witte T, et al (2012) Genetic association of miRNA-146a with systemic lupus erythematosus in Europeans through decreased expression of the gene. *Genes Immun* 13: 268–274. <https://doi.org/10.1038/gene.2011.84> PMID: 22218224
14. Roldan V, Arroyo AB, Salloum-Asfar S, Manzano-Fernandez S, Garcia-Barbera N, Marin F, et al (2014) Prognostic role of MIR146A polymorphisms for cardiovascular events in atrial fibrillation. *Thromb Haemost* 112: 781–788. <https://doi.org/10.1160/TH14-01-0092> PMID: 25008481
15. Tabas I, Garcia-Cardena G, Owens GK (2015) Recent insights into the cellular biology of atherosclerosis. *J Cell Biol* 209: 13–22. <https://doi.org/10.1083/jcb.201412052> PMID: 25869663
16. Guo L, Chen CH, Zhang LL, Cao XJ, Ma QL, Deng P, et al (2015) IRAK1 mediates TLR4-induced ABCA1 downregulation and lipid accumulation in VSMCs. *Cell Death Dis* 6: e1949. <https://doi.org/10.1038/cddis.2015.212> PMID: 26512959
17. Perez-Sanchez C, Aguirre MA, Ruiz-Limon P, Barbarroja N, Jimenez-Gomez Y, de la Rosa IA, et al (2016) 'Atherothrombosis-associated microRNAs in Antiphospholipid syndrome and Systemic Lupus Erythematosus patients'. *Sci Rep* 6: 31375. <https://doi.org/10.1038/srep31375> PMID: 27502756
18. Li K, Ching D, Luk FS, Raffai RL (2015) Apolipoprotein E enhances microRNA-146a in monocytes and macrophages to suppress nuclear factor-kappaB-driven inflammation and atherosclerosis. *Circ Res* 117: e1–e11. <https://doi.org/10.1161/CIRCRESAHA.117.305844> PMID: 25904598
19. Fuster JJ, Gonzalez-Navarro H, Vinue A, Molina-Sanchez P, Andres-Manzano MJ, Nakayama KI, et al (2011) Deficient p27 phosphorylation at serine 10 increases macrophage foam cell formation and aggravates atherosclerosis through a proliferation-independent mechanism. *Arterioscler Thromb Vasc Biol* 31: 2455–2463. <https://doi.org/10.1161/ATVBAHA.111.235580> PMID: 21885849
20. Diez-Juan A, Andres V (2001) The growth suppressor p27(Kip1) protects against diet-induced atherosclerosis. *FASEB J* 15: 1989–1995. <https://doi.org/10.1096/fj.01-0130com> PMID: 11532979
21. Rius C, Sanz MJ (2015) Intravital Microscopy in the Cremaster Muscle Microcirculation for Endothelial Dysfunction Studies. *Methods Mol Biol* 1339: 357–366. [https://doi.org/10.1007/978-1-4939-2929-0\\_26](https://doi.org/10.1007/978-1-4939-2929-0_26) PMID: 26445803
22. Cheng HS, Besla R, Li A, Chen Z, Shikatani EA, Nazari-Jahantigh M, et al (2017) Paradoxical Suppression of Atherosclerosis in the Absence of microRNA-146a. *Circ Res* 121: 354–367. <https://doi.org/10.1161/CIRCRESAHA.116.310529> PMID: 28637783
23. Andreou I, Sun X, Stone PH, Edelman ER, Feinberg MW (2015) miRNAs in atherosclerotic plaque initiation, progression, and rupture. *Trends Mol Med* 21: 307–318. <https://doi.org/10.1016/j.molmed.2015.02.003> PMID: 25771097
24. Boldin MP, Taganov KD, Rao DS, Yang L, Zhao JL, Kalwani M, et al (2011) miR-146a is a significant brake on autoimmunity, myeloproliferation, and cancer in mice. *J Exp Med* 208: 1189–1201. <https://doi.org/10.1084/jem.20101823> PMID: 21555486
25. Kanters E, Pasparakis M, Gijbels MJ, Vergouwe MN, Partouns-Hendriks I, Fijneman RJ, et al (2003) Inhibition of NF-kappaB activation in macrophages increases atherosclerosis in LDL receptor-deficient mice. *J Clin Invest* 112: 1176–1185. <https://doi.org/10.1172/JCI18580> PMID: 14561702
26. Gareus R, Kotsaki E, Xanthouleas S, van dM I, Gijbels MJ, Kardakaris R, et al (2008) Endothelial cell-specific NF-kappaB inhibition protects mice from atherosclerosis. *Cell Metab* 8: 372–383. <https://doi.org/10.1016/j.cmet.2008.08.016> PMID: 19046569

27. Polykratis A, van LG, Xanthoulea S, Hellmich M, Pasparakis M (2012) Conditional targeting of tumor necrosis factor receptor-associated factor 6 reveals opposing functions of Toll-like receptor signaling in endothelial and myeloid cells in a mouse model of atherosclerosis. *Circulation* 126: 1739–1751. <https://doi.org/10.1161/CIRCULATIONAHA.112.100339> PMID: 22935568
28. Cheng HS, Sivachandran N, Lau A, Boudreau E, Zhao JL, Baltimore D, et al (2013) MicroRNA-146 represses endothelial activation by inhibiting pro-inflammatory pathways. *EMBO Mol Med* 5: 949–966.
29. Ma S, Tian XY, Zhang Y, Mu C, Shen H, Bismuth J, et al (2016) E-selectin-targeting delivery of micro-RNAs by microparticles ameliorates endothelial inflammation and atherosclerosis. *Sci Rep* 6: 22910. <https://doi.org/10.1038/srep22910> PMID: 26956647
30. Sun X, Icli B, Wara AK, Belkin N, He S, Kobzik L, et al (2012) MicroRNA-181b regulates NF-kappaB-mediated vascular inflammation. *J Clin Invest* 122: <https://doi.org/10.1172/JCI61495> PMID: 22622040
31. Xiang Y, Cheng J, Wang D, Hu X, Xie Y, Stitham J, et al (2015) Hyperglycemia repression of miR-24 coordinately upregulates endothelial cell expression and secretion of von Willebrand factor. *Blood* 125: 3377–3387. <https://doi.org/10.1182/blood-2015-01-620278> PMID: 25814526
32. Lin N, An Y (2017) Blockade of 146b-5p promotes inflammation in atherosclerosis-associated foam cell formation by targeting TRAF6. *Exp Ther Med* 14: 5087–5092. <https://doi.org/10.3892/etm.2017.5121> PMID: 29201219